PHYSICAL REVIEW B **82**, 155120 (2010)

Visualizing elusive phase transitions with geometric entanglement

Román Orús[1] and Tzu-Chieh Wei[2]
[1]*School of Mathematics and Physics, The University of Queensland, Queensland 4072, Australia*
[2]*Department of Physics and Astronomy, University of British Columbia, Vancouver, British Columbia, Canada V6T 1Z1*
(Received 30 June 2010; published 13 October 2010)

We show that by examining the global geometric entanglement it is possible to identify "elusive" or hard to detect quantum phase transitions. We analyze several one-dimensional quantum spin chains and demonstrate the existence of nonanalyticities in the geometric entanglement, in particular, across a Kosterlitz-Thouless transition and across a transition for a gapped deformed Affleck-Kennedy-Lieb-Tasaki chain. The observed nonanalyticities can be understood and classified in connection to the nature of the transitions, and are in sharp contrast to the analytic behavior of all the two-body reduced density operators and their derived entanglement measures.

DOI: 10.1103/PhysRevB.82.155120 PACS number(s): 64.70.Tg, 03.65.Ud, 03.67.Hk, 75.10.Jm

I. INTRODUCTION

The effect of interactions in many-body systems gives rise to striking collective phenomena.[1] Phase transitions, both classical and quantum, are the archetypical example. Across such a transition, collective properties of the system undergo abrupt changes that can sometimes be related to nonanalytic behavior of the free energy. This observation was at the basis of the first historical attempt to classify phase transitions by Ehrenfest, according to the *order* of the nonanalyticity involved. Modern classification schemes have refined this idea in order to include new types of transitions.[1,2]

Across quantum phase transitions (QPT), one expects that the ground-state wave function undergoes drastic changes and hence manifests this behavior via physical quantities such as correlations. Recently there has been a significant effort toward exploring the relation between the revived quantum-mechanical entanglement and QPT (Ref. 3) to complement traditional approaches. For instance, important scaling properties have been found for the entanglement entropy and single-copy entanglement between macroscopic regions in various contexts,[4] including the connection to the central charge. A different approach has been the use of entanglement between individual constituents, such as the two-qubit concurrence[5] and other correlation-based measures.[6] In particular, concurrence was demonstrated to display singularity across QPT.[5] It was later recognized that such nonanalytic behavior originates in the two-body reduced density matrices and is linked to the nonanalyticity in the ground-state energy (the so-called "generalized Hohenberg-Kohn Theorem").[7] Also, a similar approach (but not originated from entanglement) called fidelity measure, which employs the overlap between two ground states, has been successful in identifying QPT.[8]

According to the above picture, it is possible to detect finite-order transitions just by examining the nonanalyticities of two-body entanglement measures. However, one encounters difficulty with other types of transitions. For instance, in ∞-order transitions, such as Kosterlitz-Thouless (KT), the ground-state energy and its derivatives are analytic, as well as all correlation functions, such as two-body observables. This is the case of, e.g., the spin-1/2 XXZ chain near the antiferromagnetic Heisenberg point. A further example, not of the KT type, is a transition occurring in a deformed Affleck-Kennedy-Lieb-Tasaki (AKLT) chain introduced by Verstraete *et al.* in Ref. 9, where the existence of a diverging *entanglement length scale* in the system remains undetected by any correlation functions of the ground state, as the system is always gapped and the correlation length remains finite. The complex nature of these transitions makes them elusive and undetectable by all the above entanglement approaches (as well as the fidelity susceptibility measure),[10] and previous investigations indicate that they may be better understood in terms of *global* quantities.[11–13]

Here we provide a perspective along this direction, and show that for one-dimensional (1D) quantum many-body systems *the global geometric entanglement can be used to successfully detect QPT, including finite-order and the above elusive ones*. The geometric entanglement (GE) (Ref. 14) has previously been shown to exhibit divergence consistent with a scaling hypothesis,[15,16] and has also been related to the central charge of the underlying conformal theories at criticality.[17] Moreover, its finite-size corrections at criticality are also governed by conformal symmetry.[15] In this context, the aim of the present work is to show that even when all correlation functions remain analytic, the GE is still able to display singularity across transitions. We shall also elaborate on the connection between the origin of these singularities and the nature of the observed transitions.

The structure of this paper is as follows: in Sec. II we review briefly the basics on the global geometric entanglement. In Sec. III we show our results for a variety of 1D systems, namely, the spin-1/2 Ising model in transverse and longitudinal fields, the spin-1/2 XXZ model, and the deformed AKLT model. Section IV offers a discussion of the results focusing on two aspects: first, the connection between the observed singularities for the GE and the nature of the phase transitions, and second, a comparison of the performance to detect QPTs between the GE and other entanglement-related quantities. Finally, Sec. V contains the conclusions.

II. GLOBAL GEOMETRIC ENTANGLEMENT PER SITE

In this section we briefly remind the basics of the global geometric entanglement. To characterize *global* entangle-

ment, consider a general, N-partite, normalized pure state $|\Psi\rangle \in \mathcal{H}=\otimes_{i=1}^{N}\mathcal{H}^{[i]}$, where $\mathcal{H}^{[i]}$ is the Hilbert space of party i. For a spin system each party could be a single spin but could also be a block of contiguous spins.[14–17] Our scheme involves considering how well an entangled state can be approximated by some unentangled (normalized) state: $|\Phi\rangle \equiv \otimes_{i=1}^{N}|\phi^{[i]}\rangle$, motivated by mean-field theory. For quantum spin systems, the mean-field scheme attempts to find the best product state $|\Phi\rangle$ minimizing the Hamiltonian H. Here, we aim to find the best mean-field approximation to the ground state $|\Psi\rangle$. The proximity of $|\Psi\rangle$ to $|\Phi\rangle$ is captured by their overlap; the entanglement of $|\Psi\rangle$ is revealed by the maximal overlap[14]

$$\Lambda_{\max}(\Psi) \equiv \max_{\Phi}|\langle\Phi|\Psi\rangle|. \tag{1}$$

Λ is thus related to the best mean-field energy of the "reduced" Hamiltonian

$$H_{\text{red}} \equiv -|\Psi\rangle\langle\Psi| \tag{2}$$

as the closest product state $|\Phi^*\rangle$ is the best mean-field state such that

$$\min_{\Phi}\langle\Phi|\mathcal{H}_{\text{red}}|\Phi\rangle = \langle\Phi^*|H_{\text{red}}|\Phi^*\rangle = -\Lambda_{\max}(\Psi)^2. \tag{3}$$

It makes sense to quantify the entanglement via the following *extensive* quantity[15,16] (analogous to the relation between the free energy and the partition function)

$$E(\Psi) \equiv -\log_2 \Lambda_{\max}^2(\Psi), \tag{4}$$

where we have taken the base-2 logarithm. GE gives zero for unentangled states and is a measure of how difficult it is to approximate a given state (in particular, the ground state) by mean-field states, or equivalently a measure of unfactorizability. To deal with large systems we define the thermodynamic entanglement density $\mathcal{E}$ and its finite-size version $\mathcal{E}_N$ by

$$\mathcal{E} \equiv \lim_{N\to\infty}\mathcal{E}_N, \quad \mathcal{E}_N \equiv \frac{E(\Psi)}{N}. \tag{5}$$

This is the quantity that will be of interest in this paper.

III. VISUALIZING DIFFERENT TYPES OF TRANSITIONS

In this section we provide an analysis of different 1D quantum spin systems undergoing different types of QPTs, from the point of view of the GE. Specifically, we focus on the spin-1/2 Ising model in transverse and longitudinal fields, the spin-1/2 XXZ model, and the deformed AKLT model. Let us mention that the global geometric entanglement per site $\mathcal{E}$ has already been applied to ground states of 1D models across different types of phase transitions.[15–17] Our analysis here complements those from previous studies by offering results in more exotic situations.

A. Spin-1/2 Ising model

For comparative purposes, we first revisit the spin-1/2 quantum Ising model in transverse and longitudinal fields

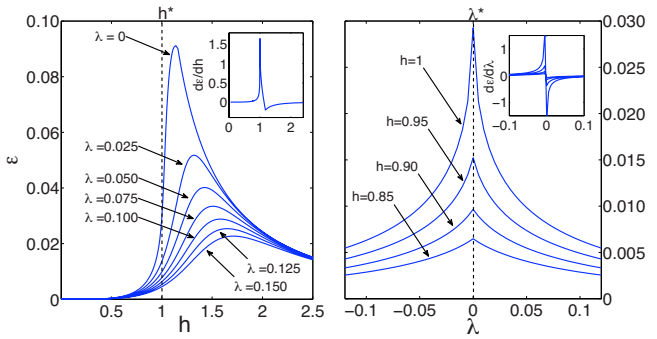

FIG. 1. (Color online) $\mathcal{E}$ for the Ising model obtained with MPS vs the transverse field h for several values of the longitudinal field λ (left) and vs the longitudinal field λ for several values of the transverse field h (right). The insets show the derivatives with respect to h and λ. The derivative $d\mathcal{E}/dh$ in the left panel corresponds to the line for $\lambda=0$.

$$H = -\sum_i (\sigma_x^{[i]}\sigma_x^{[i+1]} + h\sigma_z^{[i]} + \lambda\sigma_x^{[i]}), \tag{6}$$

where $h(\lambda)$ is the transverse (longitudinal) field, and $\sigma_\alpha^{[k]}$ is the αth Pauli matrix at site k. This Hamiltonian has a $\mathbb{Z}_2$ symmetry-breaking second-order quantum phase transition at $h^*=\pm 1$ and $\lambda=0$, whereas at fixed $|h|<1$ it has a first-order discontinuous transition at $\lambda^*=0$ due to a crossing of energy levels. Namely, the phase diagram is a first-order line terminated by second-order points. For this model, we employ the infinite time evolving block decimation (TEBD) algorithm[18] to find a matrix product state (MPS) approximation to the ground state in the thermodynamic limit. Then, GE is readily obtained from the MPS state by maximizing the overlap in Eq. (1) with standard optimization.

Results for the ground state of the quantum Ising model in Eq. (6) are shown in Fig. 1. On the left panel we extend the results from Ref. 16 for GE across the quantum phase transition as a function of the transverse field h for different values of λ. We have checked that our MPS results for $\lambda=0$ reproduce accurately the exact solution in Ref. 16 (less than 1% of relative error). Notice that, at $\lambda=0$, $\mathcal{E}$ is smooth across the second-order phase transition with a peak slightly after the quantum-critical point (around $h\sim 1.13$). The derivative, however, is divergent at the quantum-critical point $h=h^*=1$, as shown in the inset, and obeys the critical scaling law

$$\frac{\partial\varepsilon}{\partial h}(\lambda=0,h) \sim -\frac{1}{2\pi}\log_2|h-1| \tag{7}$$

for $|h-1|\ll 1$.[16] Also, as can be easily inferred from Fig. 1, our MPS results prove that this derivative is smooth for $\lambda\neq 0$, as there is no transition. The behavior of $\mathcal{E}$ is rather different across the line of the first-order transition as a function of the longitudinal field λ, for which we give our results in the right panel of Fig. 1. There, we see that $\mathcal{E}$ has a kink (thus being nonanalytic) as a function of λ at the first-order (discontinuous) phase transition point $\lambda=\lambda^*=0$ for $h\neq 0,1$. At the second-order phase transition point $\lambda=0$, $h=1$ our

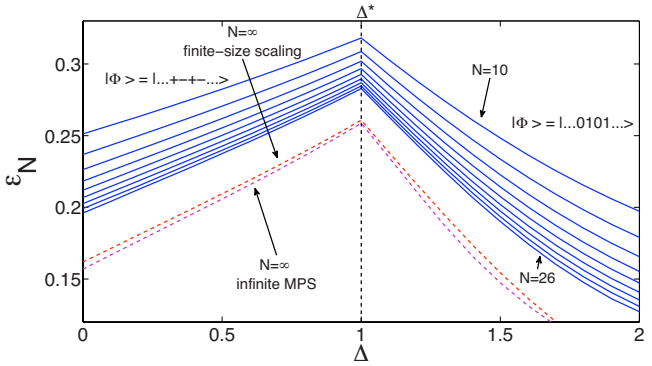

FIG. 2. (Color online) $\mathcal{E}_N$ for the XXZ model in zero field vs the anisotropy parameter Δ for system sizes $N=10$, 12, 14, 16, 18, 20, 24, and 26. The dashed lines correspond to the thermodynamic limit $\mathcal{E}$, obtained by fitting the finite-size scaling law in $\mathcal{E}_N(\Delta) \sim \mathcal{E}(\Delta) + b(\Delta)/N$ (upper dashed line) and by the infinite MPS method (lower line). We also indicate the closest product state $|\Phi\rangle$ on each side.

MPS results are compatible with a logarithmic divergence of the derivative

$$\frac{\partial \varepsilon}{\partial \lambda}(\lambda, h=1) \sim -a \log_2|\lambda| \tag{8}$$

for $|\lambda| \ll 1$, with $a \sim -7.5(1)$. Notice that $\mathcal{E}$ is symmetric around $\lambda=\lambda^*$ since at this point the Hamiltonian is self-dual under the duality transformation $\lambda \to -\lambda$. The observed nonanaliticity at $\lambda=0$ and $h \neq 0,1$ can be understood as a consequence of a global change in the ground-state wave function, characteristic of first-order transitions with a crossing of ground state energy levels. What is more intriguing is that similar nonanalytical behaviors in $\mathcal{E}$ are also found in other types of transitions, even continuous ones, as we will see in what follows.

B. Spin-1/2 XXZ model

We now consider a system with an elusive phase transition, i.e., the 1D spin-1/2 XXZ model

$$H = \sum_i (\sigma_x^{[i]}\sigma_x^{[i+1]} + \sigma_y^{[i]}\sigma_y^{[i+1]} + \Delta\sigma_z^{[i]}\sigma_z^{[i+1]} + h\sigma_z^{[i]}), \tag{9}$$

where Δ is an anisotropy parameter and h a magnetic field.

Let us first study the case of zero field ($h=0$). In this regime, this model is critical for $\Delta \in (-1,1]$, with a KT quantum phase transition at the Heisenberg point $\Delta^*=1$.[19] Within this setting, first we do an exact diagonalization of H for sizes up to 26 spins and find the geometric entanglement, followed by a finite-size scaling and extrapolation to the thermodynamic limit. Then we compare this value with that obtained by using the MPS method for infinite systems, as used for the quantum Ising model. In turn, this allows us to further validate the consistency of our numerical methods.

In Fig. 2 we show the results for the spin-1/2 XXZ model in Eq. (9) in zero field. We see that the global geometric entanglement per site $\mathcal{E}_N$ for finite size N already displays a pronounced kink at the KT quantum critical point $\Delta=\Delta^*=1$.

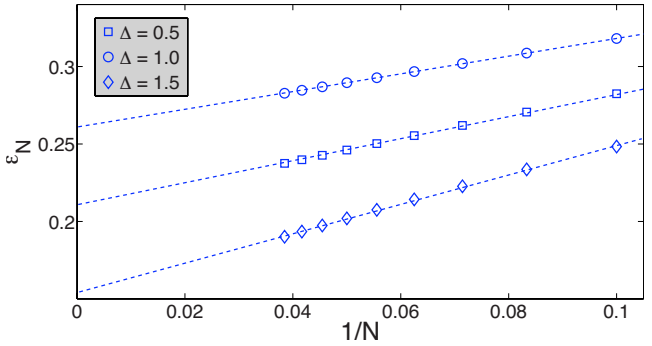

FIG. 3. (Color online) $\mathcal{E}_N$ for the spin-1/2 XXZ model in zero field, as a function of $1/N$ for system sizes $N=10$, 12, 14, 16, 18, 20, 24, and 26. The data correspond to $\Delta=0.5$, 1, and 1.5. The dashed lines are our best fits to Eq. (10). The values extrapolated to the thermodynamic limit $1/N \to 0$ correspond to those of the dashed line plotted in Fig. 2.

As observed in the figure, $\mathcal{E}_N$ seems to converge fast toward a thermodynamic value as N increases. Our finite-size scaling analysis indicates a scaling law

$$\mathcal{E}_N(\Delta) \sim \mathcal{E}(\Delta) + \frac{b(\Delta)}{N} \tag{10}$$

in good agreement with the ones proposed in Ref. 15, see Fig. 3.

We have done this scaling analysis for all the computed values of Δ and obtained an estimation of the thermodynamic quantity $\mathcal{E}$, shown in Fig. 2, together with the infinite MPS estimation and the finite-size data. The values of $\mathcal{E}$ estimated by both methods agree within 1% of relative error, which validates the consistency of our different approaches. The kink in $\mathcal{E}_N$ at $\Delta=1$ is obviously present in the thermodynamic limit $N \to \infty$. This is a remarkable result, as for this KT transition all the two-body observables and all their derivatives are analytic, and this means that entanglement measures that only depend on two-body reduced density operators, such as the concurrence and the spin-spin negativity, will *not* exhibit any singularity at all. Our results also indicate that this kink is due to a sudden change in the product state that maximizes the overlap in Eq. (1): for $\Delta<1$ the closest product state $|\Phi\rangle$ is $|\cdots+-+-\cdots\rangle$ (as well as those from rotating $|\cdots+-+-\cdots\rangle$ around z axis, due to SO(2) symmetry), whereas for $\Delta>1$ it is $|\ldots0101\ldots\rangle$ (where $|\pm\rangle \equiv (|0\rangle \pm |1\rangle)/\sqrt{2}$, and $|0\rangle$ and $|1\rangle$ are the eigenstates of σ_z). At the isotropic point $\Delta=1$, either of the two product states is equally good, due to the SU(2) symmetry. The observed kink in the global geometric entanglement evidences the existence of the KT transition and its similitude with the nonanalytical behavior found in discontinuous phase transitions (see Fig. 1) supports the fact that there is a *sudden and global* change in the structure of the ground-state wave function.[20] Notice, though, that according to the standard classification, *the phase transition in this model is continuous*.

Let us now consider the case of nonzero field ($h \neq 0$) in the Hamiltonian. In this generic case, by looking at the discontinuities in the GE, we find out that it is also possible to get both a qualitative and quantitative picture of the correct

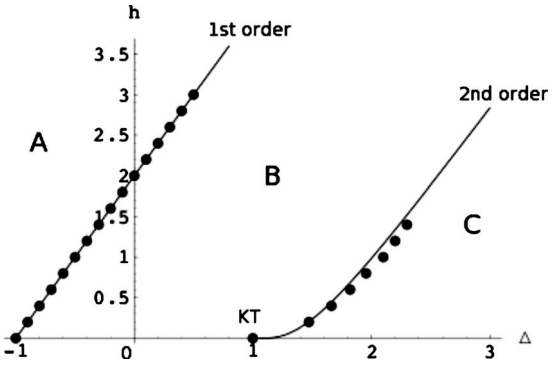

FIG. 4. Phase diagram of the XXZ model from Eq. (9) in the (h,Δ) plane. The dots correspond to our estimation observing the discontinuities of the GE using MPS methods for infinite systems and the lines are the exact phase boundaries. Phases A and C are gapped whereas phase B is gapless. Phases A and B are separated by a line of first order transitions whereas phases B and C are separated by a line of second-order transitions at $h>0$ that ends in a KT transition at $h=0$.

phase diagram for this model in the (h,Δ) plane. Our results for the phase diagram estimated using the GE obtained from MPS methods for infinite systems are shown in Fig. 4. As seen in the plot, there is a good quantitative agreement between the phase boundaries estimated with the GE and the exact ones (computed by Bethe ansatz). Thus, we see that the GE is able to reproduce within good accuracy the correct properties of the phase diagram of the model.

C. Deformed AKLT model

Finally, we consider the deformed AKLT model[9]

$$H = \sum_i X_\mu^{[i,i+1]},$$

$$X_\mu^{[i,i+1]} = [(\Sigma_\mu^{[i]})^{-1} \otimes \Sigma_\mu^{[i+1]}] X_{\mathrm{AKLT}}^{[i,i+1]} [(\Sigma_\mu^{[i]})^{-1} \otimes \Sigma_\mu^{[i+1]}], \tag{11}$$

where $\Sigma_\mu^{[i]} \equiv \mathbb{I}^{[i]} + \sinh(\mu) S_z^{[i]} + [\cosh(\mu) - 1](S_z^{[i]})^2$ and

$$X_{\mathrm{AKLT}}^{[i,i+1]} = \vec{S}^{[i]} \cdot \vec{S}^{[i+1]} + \frac{1}{3}(\vec{S}^{[i]} \cdot \vec{S}^{[i+1]})^2 + \frac{2}{3} \tag{12}$$

is the usual AKLT two-body term[21] with $S_\alpha^{[k]}$ the αth component of the spin-1 operator $\vec{S}^{[k]}$. The ground state undergoes a transition at the AKLT point $\mu^*=0$ with diverging entanglement length and finite correlation length. For this model, we use the exact MPS representation of the ground state from Ref. 9 and then extract from it the geometric entanglement per site in the thermodynamic limit by using the exact MPS techniques developed in the second paper of Ref. 15. For convenience of the calculation, now we choose each party in Eq. (5) to be composed by a block of two contiguous spins so that $\mathcal{E}$ now refers to the geometric entanglement per block of two spins in the thermodynamic limit.[22]

From Fig. 5 we see that GE $\mathcal{E}$ has a pronounced kink at the AKLT point $\mu=\mu^*=0$ in the thermodynamic limit, similar to that in the KT transition of the XXZ model and the first-order transition of the Ising spin chain in a longitudinal field. This similitude supports again the idea of a sudden global change in the ground-state wave function. However, notice that as explained in Ref. 9, here the system is *always gapped* and the correlation length of the ground state of the system is always smooth and remains finite for this transition. Thus, this sort of transition does not even exist according to the standard criteria and two-body correlation functions are unable to detect the observed nonanalyticity. However, the entanglement length diverges at the AKLT point.[9] Remarkably, we see here that GE is also successful in identifying the existence of this transition in the ground state of the system. We also determine the closest product state

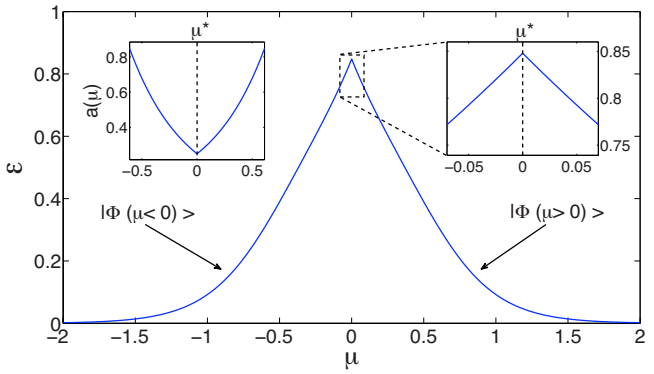

FIG. 5. (Color online) $\mathcal{E}$ for blocks of two spins for the deformed AKLT model vs the deformation parameter μ. The right inset shows a close-up around the AKLT point $\mu^*=0$ and the left inset shows the coefficient $a(\mu)$ associated with the closet product state $|\Phi(\mu)\rangle$ (see text). These results are exact.

$$|\Phi(\mu)\rangle = \left\{ C(\mu) \left[a(\mu)|0,0\rangle + \frac{1}{2}|x(\mu)\rangle \right] \right\}^{\otimes\infty} \tag{13}$$

with

$$|x(\mu \le 0)\rangle = |-1,-1\rangle, \quad |x(\mu \ge 0)\rangle = |1,1\rangle \tag{14}$$

$C(\mu)$ a normalization constant, $a(\mu)$ a real positive coefficient (see Fig. 5), and $|-1\rangle$, $|0\rangle$, and $|1\rangle$ the eigenstates of the spin-1 operator S_z.

IV. DISCUSSION

The results obtained in the previous section prove the usefulness of the GE to detect phase transitions of many different kinds, including those that seem difficult to detect with alternative methods. In this section we discuss a number of important considerations that can be observed from our results, namely, (i) how do the singularities in GE connect to the nature of the transitions and (ii) how does the GE compare to other alternative measures in efficiency of calculations and visualization of results.

A. Singularities in GE and the nature of the transitions

To illustrate the nature of the observed singularities in the GE, consider for simplicity spin-1/2 systems and rewrite the N-spin product state $|\Phi\rangle$ via

$$|\Phi\rangle\langle\Phi| = \bigotimes_{i=1}^{N} \frac{1}{2}(\mathbb{1}^{[i]} + \vec{r}^{[i]} \cdot \vec{\sigma}^{[i]}), \tag{15}$$

where the unit vectors $\vec{r}^{[i]}$'s represent directions of local spins. The overlap $|\langle\Psi|\Phi\rangle|^2$ can be expressed (by expanding the above product) as a linear combination of all correlations with respect to $|\Psi\rangle$

$$2^N|\langle\Phi|\Psi\rangle|^2 = 1 + \sum_i \vec{r}^{[i]} \cdot \langle\vec{\sigma}^{[i]}\rangle + \sum_{i\neq j,\alpha,\beta} r_\alpha^{[i]} r_\beta^{[j]} \langle\sigma_\alpha^{[i]}\sigma_\beta^{[j]}\rangle + \sum_{i\neq j\neq k,\alpha,\beta,\gamma} r_\alpha^{[i]} r_\beta^{[j]} r_\gamma^{[k]} \langle\sigma_\alpha^{[i]}\sigma_\beta^{[j]}\sigma_\gamma^{[k]}\rangle + \cdots . \tag{16}$$

This can be easily generalized to systems of higher spins. Therefore, it is seen that a singularity of the entanglement can come from two types of sources: (i) correlation functions, $\mathcal{C}_{\alpha,\beta,\gamma,\ldots}^{[i,j,k,\ldots]} \equiv \langle\sigma_\alpha^{[i]}\sigma_\beta^{[j]}\sigma_\gamma^{[k]}\ldots\rangle$ for the ground state $|\Psi\rangle$ and (ii) parameters $\vec{r}^{*[i]}$, which denote the vectors that maximize the overlap.

In all the examples that we have examined, we can classify the origin of the singularity due to (i) or (ii) or both. Let us summarize: (1) for the transverse Ising model, which has a standard second-order quantum critical point, (i) correlation functions $\mathcal{C}$'s are singular but (ii) optimal parameters r^*'s are not singular. This explains the similar behavior between the GE and the so-called concurrence measure of entanglement, which depends on correlation functions. (2) For the longitudinal Ising model, which has a standard first-order transition, both (i) and (ii) are singular, as the transition is first-order. (3) For the XXZ model at zero field, the transition is ∞ order, therefore (i) correlations $\mathcal{C}$'s are not singular, but (ii) the parameters r^*'s of the optimal local states are singular. It is this second point the one that helps to signify certain nonanalytic change in the wave function and thus identifies the transition. (4) For the deformed AKLT model, (i) correlations $\mathcal{C}$'s are not singular, since the correlation length is finite, but (ii) r^*'s are singular. Similar to XXZ, it is this second point the one that detects nonanalyticity in the wave function across the transition.

B. Comparison to correlation functions

Let us now discuss the relevance of the GE as compared to other approaches based on correlation functions to study phase transitions. One could be tempted to affirm that any phase transition, if it exists, can, in principle, be detected by measuring all the possible correlation functions of the system, and that therefore the GE offers no true extra information and is not useful to study phase transitions.

We argue here that this approach may not actually apply. To see this, first notice that it is impractical to exhaust all possible correlations to find out if there is any singularity in a given system. And moreover, there exist example Hamiltonians where all the ground-state correlations are well behaved and no singularity can be found (e.g., XXZ model at $h=0$). Entanglement measures that depend on correlation functions, such as the concurrence, also inherit this analytical behavior. Therefore, a quantity which includes all the possible correlation functions in a single quantity is potentially very useful as one then would need to examine this single quantity to see if any singularity exists in the correlations. As shown above, one has that (i) the GE is actually such a quantity since it can be expressed in terms of a combination of all possible correlation functions (general k-point correlations) and (ii) there are additional quantities (e.g., the vectors that characterize the best local product state) that also assist the examination of singularities. In all our examples examined in the paper, we can classify the origin of the singularity is due to (i) or (ii) or both. In short, GE is a simple and meaningful quantity that provides information that cannot be codified in any (local) correlation function and the approach is clearly more efficient than calculating all possible correlation functions and examining them one by one.

C. Comparison to other measures: Localizable entanglement, entropy, and fidelity

Let us now briefly discuss how the GE compares to other entanglement-related quantities in detecting phase transitions. We focus on the localizable entanglement, the entanglement entropy, and the ground-state fidelity. Notice that of all these quantities, the fidelity is not a measure of entanglement by itself. We remark, however, that this does not diminish its usefulness in studying phase transitions.

Let us first considered the appearance of singular behaviors across QPTs. Quite importantly, for the two elusive models studied in this work (XXZ and deformed AKLT), measures such as the entanglement entropy and fidelity measures[10] (which we also analyzed for deformed AKLT—results not shown) fail to show any singularity across the transitions. Furthermore, if one considers a derived quantity from fidelity, called fidelity susceptibility, it can be shown that for KT transition it does not show any singularity.[10] The localizable entanglement, however, shows a singular behavior in these two transitions as well,[9,12] in a way similar to the one observed with the GE. Notice, though, that the GE may be easier to compute than the localizable entanglement in many cases, as we argue below.

Next, let us consider the efficiency in the calculation of the different measures. For certain exactly solvable models, the GE can be calculated essentially analytically. Furthermore, for nonsolvable models, with existing numerical techniques based on tensor networks such as MPS or projected entangled pair state (PEPS) (Ref. 23) it is rather straightforward to compute the GE.

In fact, the geometric entanglement is probably one of the multipartite entanglement measures that is easier to calculate while most of the other known multipartite entanglement measures end up being rather hard to compute. For example, in the framework of MPS, computing GE is not harder than computing the ground state. Once we have a MPS approximation of the ground state, it is numerically easy to calculate the GE, i.e., we take bond dimension 1 in an MPS that minimizes the energy of the Hamiltonian $H' = -|\Psi\rangle\langle\Psi|$, where $|\Psi\rangle$ is the MPS ground state approximation of the original Hamiltonian under study. Comparing to other approaches, we note that the calculation of the fidelity susceptibility also

requires the knowledge of ground states but is perhaps more inefficient than our approach from a computational point of view, as it would require the overlap between two MPS instead of an MPS and a product state. Regarding the entanglement entropy, its calculation requires computing the reduced density matrix of a block of finite size together with its spectrum, which cannot always be done efficiently (especially for systems in more than one dimension). Finally, regarding the localizable entanglement, there is, in general, the necessity to maximize over all possible local measurements (not necessary projective measurements), which makes it the most difficult calculation of all the ones discussed so far for a generic model.

V. CONCLUSIONS

Here we have shown that the global geometric entanglement can be used to successfully detect conventional and elusive phase transitions, such as the ones for the 1D spin-1/2 Ising, XXZ and deformed spin-1 AKLT models. We have also clarified the connection between the nature of the observed transitions and the fact that the geometric entanglement exhibits singularities whereas other entanglement measures do not. Thus, we have demonstrated that the GE can be used to detect elusive transitions for which other conventional methods and other entanglement measures (including the fidelity susceptibility between ground states) fail.

All in all, we believe that the GE may provide complementary information about the complicated ground states of quantum many-body systems to the one offered by alternative measures such as, e.g., correlation functions, entanglement entropy, localizable entanglement, and ground-state fidelity. However, there is still lack of extensive study of the relations among all these methods. Further study in this direction would help to clarify the complex nature of the ground state of strongly correlated systems.

ACKNOWLEDGMENTS

R.O. acknowledges financial support from the ARC and the University of Queensland. T.-C.W. acknowledges support from NSERC and MITACS.

[1] See, e.g., X.-G. Wen, *Quantum Field Theory of Many-Body Systems* (Oxford University Press, Oxford, 2004).
[2] J. M. Kosterlitz and D. J. Thouless, J. Phys. C **6**, 1181 (1973).
[3] See, e.g., L. Amico, R. Fazio, A. Osterloh, and V. Vedral, Rev. Mod. Phys. **80**, 517 (2008).
[4] G. Vidal, J. I. Latorre, E. Rico, and A. Kitaev, Phys. Rev. Lett. **90**, 227902 (2003); J. I. Latorre, E. Rico, and G. Vidal, Quantum Inf. Comput. **4**, 48 (2004); V. E. Korepin, Phys. Rev. Lett. **92**, 096402 (2004); A. R. Its, B. Q. Jin, and V. E. Korepin, J. Phys. A **38**, 2975 (2005); P. Calabrese and J. Cardy, J. Stat. Mech.: Theory Exp. (2004) P06002; M. B. Plenio, J. Eisert, J. Dreissig, and M. Cramer, Phys. Rev. Lett. **94**, 060503 (2005); M. M. M. Wolf, *ibid.* **96**, 010404 (2006); J. Eisert and M. Cramer, Phys. Rev. A **72**, 042112 (2005); I. Peschel and J. Zhao, J. Stat. Mech.: Theory Exp. (2005) P11002; R. Orús, J. I. Latorre, J. Eisert, and M. Cramer, Phys. Rev. A **73**, 060303(R) (2006); A. Riera and J. I. Latorre, *ibid.* **74**, 052326 (2006).
[5] A. Osterloh, L. Amico, G. Falci, and R. Fazio, Nature (London) **416**, 608 (2002); T. J. Osborne and M. A. Nielsen, Phys. Rev. A **66**, 032110 (2002).
[6] X. Cui, S. J. Gu, J. Cao, Y. Wang, and H.-Q. Lin, J. Phys. A **40**, 13523 (2007).
[7] L.-A. Wu, M. S. Sarandy, and D. A. Lidar, Phys. Rev. Lett. **93**, 250404 (2004); L.-A. Wu, M. S. Sarandy, D. A. Lidar, and L. J. Sham, Phys. Rev. A **74**, 052335 (2006); L. Campos Venuti, C. Degli Esposti Boschi, M. Roncaglia, and A. Scaramucci, *ibid.* **73**, 010303(R) (2006).
[8] P. Zanardi and N. Paunković, Phys. Rev. E **74**, 031123 (2006); H. Zhou and J. Barjaktarevic, arXiv:cond-mat/0701608 (unpublished); P. Buonsante and A. Vezzani, Phys. Rev. Lett. **98**, 110601 (2007); P. Zanardi, P. Giorda, and M. Cozzini, *ibid.* **99**, 100603 (2007); H.-Q. Zhou, R. Orús, and G. Vidal, *ibid.* **100**, 080601 (2008); S. Gu, arXiv:0811.3127 (unpublished).
[9] F. Verstraete, M. A. Martín-Delgado, and J. I. Cirac, Phys. Rev. Lett. **92**, 087201 (2004).
[10] S. J. Gu, H. Q. Lin, and Y. Q. Li, Phys. Rev. A **68**, 042330 (2003); S. J. Gu, H. M. Kwok, W. Q. Ning, and H. Q. Lin, Phys. Rev. B **77**, 245109 (2008).
[11] However, if one uses the Bethe ansatz solution for the XXZ chain, the fidelity susceptibility via the bosonization technique will show singularity at transition points. See M.-F. Yang, Phys. Rev. B **76**, 180403(R) (2007).
[12] M. Popp, F. Verstraete, M. A. Martín-Delgado, and J. I. Cirac, Phys. Rev. A **71**, 042306 (2005).
[13] H. Wang, J. Zhao, B. Li, and H. Zhou, arXiv:0902.1670 (unpublished).
[14] T.-C. Wei and P. M. Goldbart, Phys. Rev. A **68**, 042307 (2003).
[15] R. Orús, S. Dusuel, and J. Vidal, Phys. Rev. Lett. **101**, 025701 (2008); R. Orús, Phys. Rev. A **78**, 062332 (2008); Q.-Q. Shi, R. Orús, J. O. Fjaerestad, and H.-Q. Zhou, New J. Phys. **12**, 025008 (2010); W. Son, L. Amico, S. Pascazio, R. Fazio, and V. Vedral, arXiv:1001.2656 (unpublished); J. Stéphan, G. Misguich, and F. Alet, arXiv:1007.4161 (unpublished); R. Orús and T.-C. Wei, arXiv:1006.5584 (unpublished).
[16] T.-C. Wei, D. Das, S. Mukhopadyay, S. Vishveshwara, and P. M. Goldbart, Phys. Rev. A **71**, 060305(R) (2005); T. Wei, *ibid.* **81**, 062313 (2010).
[17] R. Orús, Phys. Rev. Lett. **100**, 130502 (2008); A. Botero and B. Reznik, arXiv:0708.3391 (unpublished).
[18] G. Vidal, Phys. Rev. Lett. **98**, 070201 (2007); R. Orús and G. Vidal, Phys. Rev. B **78**, 155117 (2008).
[19] We note that across the ferromagnetic point $\Delta=-1$, the geometric entanglement shows a discontinuity.
[20] These results are somehow similar to those observed for the localizable entanglement in this particular model (Ref. 12).
[21] I. Affleck, T. Kennedy, E. H. Lieb, and H. Tasaki, Commun. Math. Phys. **115**, 477 (1988); Phys. Rev. Lett. **59**, 799 (1987).
[22] Similar results are also obtained for other choices.
[23] J. Jordan, R. Orús, G. Vidal, F. Verstraete, and J. I. Cirac, Phys. Rev. Lett. **101**, 250602 (2008); F. Verstraete and J. Cirac, arXiv:cond-mat/0407066 (unpublished).